

Zn_{0.97}M_{0.03}O (M = Co, Fe, and V) pigments: thermal, structural, and optical characterization

T. M. Milão · J. F. A. Oliveira · V. D. Araújo ·
M. I. B. Bernardi

Received: 18 August 2010/Accepted: 13 October 2010/Published online: 4 November 2010
© Akadémiai Kiadó, Budapest, Hungary 2010

Abstract Zinc oxide is a widely used white inorganic pigment. Transition metal ions are used as chromophores and originate the ceramic pigments group. In this context, ZnO particles doped with Co, Fe, and V were synthesized by the polymeric precursors method, Pechini method. Differential scanning calorimetry (DSC) and thermogravimetry (TG) techniques were used to accurately characterize the distinct thermal events occurring during synthesis. The TG and DSC results revealed a series of decomposition temperatures due to different exothermal events, which were identified as H₂O elimination, organic compounds degradation and phase formation. The samples were structurally characterized by X-Ray diffractometry revealing the formation of single phase, corresponding to the crystalline matrix of ZnO. The samples were optically characterized by diffuse reflectance measurements and colorimetric coordinates L*, a*, b* were calculated for the pigment powders. The pigment powders presented a variety of colors ranging from white (ZnO), green (Zn_{0.97}Co_{0.03}O), yellow (Zn_{0.97}Fe_{0.03}O), and beige (Zn_{0.97}V_{0.03}O).

Keywords ZnO · Dopants · Pechini method · Pigments

Introduction

Inorganic pigments are traditionally based on transition metal compounds. Research on ceramic pigments has lately been dedicated to improve traditional colored systems from an environmental point of view and maintaining their coloring properties and technological requirements [1].

Attempting to achieve zero emissions and waste, as well as a reduction of energy costs, a good understanding of the reaction mechanisms depending on the chemical composition is required. Moreover, the product performance must meet the growing social demands with regard to safety, sustainability, and minimal environmental impact [1].

Zinc oxide (ZnO) has a wide direct band gap of 3.37 eV at room temperature and a large exciton binding energy of about 60 meV with the electrical and optical properties of a II–VI semiconductor. It has useful characteristics, such as excellent thermal and chemical stability, a large piezoelectric constant, and an easily modified electric conductivity [2].

In ZnO, the Zn atoms are tetrahedrally coordinated to four oxygen atoms, where Zn *d* electrons hybridize with the oxygen *p* electrons. The interest in determining electrical and optical properties of doped bulk ZnO is motivated by the need to develop an understanding of the material response to impurities introduced by doping [3]. Zinc oxide (ZnO) has attracted attention because of the wide range of applications such as solar cells, luminescent, electrical, and acoustic devices, as well as chemical sensors [4], varistors and pigment in paints [3].

In recent years, many techniques and methods have been investigated for the obtention of ZnO nanostructures, such as solvothermal method [5], sol–gel technique [3], solid-state reaction [6], and Pechini method [7]. Lima et al. [8] mention the different methods, such as physical and chemical vapor deposition, metal organic vapor-phase

T. M. Milão (✉) · J. F. A. Oliveira
Departamento de Química, UFSCar—Universidade Federal de São Carlos, Rodovia Washington Luiz, Km 235, São Carlos, SP 13565-905, Brazil
e-mail: thismilao@gmail.com

V. D. Araújo · M. I. B. Bernardi
Instituto de Física de São Carlos, USP—Universidade de São Paulo, Av. Trabalhador São-carlense, 400, São Carlos, SP 13560-970, Brazil

epitaxy, microwave plasma deposition, pyrolysis, chemical bath deposition, heterogeneous nucleation in mixed or/and aqueous solution, and the hydrothermal method.

This study involved the synthesis of $Zn_{1-x}M_xO$ ($M = Co, Fe$, and V) system, with $x = 0$ and 0.03 (%mol) powders and a study of their thermal behavior as a function of the structural and optical properties for pigment applications. The samples were prepared by the polymeric precursor method. This method, also called the Pechini method [9], allows for the production of nanocrystalline powder samples at relatively low temperatures. This synthesis produces a polymer network starting from a poly-hydroxy alcohol and an alpha-hydroxycarboxylic acid, with metallic cations homogeneously distributed throughout the matrix [10]. The samples were characterized by thermal analysis, thermogravimetric and differential scanning calorimetry, X-ray diffraction, diffuse reflectance, and colorimetric coordinate techniques.

Experimental procedure

The polymeric precursor method is based on the polymerization of metallic citrate using ethylene glycol. A hydrocarboxylic acid such as citric acid is normally used to chelate cations in an aqueous solution. The addition of a polyalcohol such as ethylene glycol leads to the formation of an organic ester. Polymerization promoted by heating to around $100\text{ }^{\circ}\text{C}$ results a homogenous resin in which the metal ions are distributed uniformly throughout the organic matrix. The resin is then calcined to produce the desired oxides [11].

Zinc nitrate ($Zn(NO_3)_2 \cdot 6H_2O$ —Alfa Aesar 99%), citric acid ($C_6H_8O_7 \cdot H_2O$ —Synth 99.5%), cobalt nitrate ($(Co(NO_3)_2 \cdot 6H_2O$ —Dinâmica 98%), ammonium metavanadate (NH_4VO_3 —Merck 99%), and iron II sulfate ($(Fe(SO_4)_2 \cdot 7H_2O$ —Dinâmica 98%), were used as precursors.

The zinc nitrate, citric acid, and dopants were dissolved in water and then mixed into an aqueous citric acid solution ($100\text{ }^{\circ}\text{C}$) under constant stirring. Next, ethylene glycol ($HOCH_2CH_2OH$) was added to polymerize the citrate by a polyesterification reaction. The citric acid:metal molar ratio was 3:1, while the citric acid:ethylene glycol mass ratio was 60:40. The compositions studied here are $Zn_{1-x}M_xO$ ($M = Co, Fe$, and V), where x (%mol) = 0 and 0.03. The resulting resin was calcined at $330\text{ }^{\circ}\text{C}$ for 30 min at $10\text{ }^{\circ}\text{C}/\text{min}$, leading to the formation of the precursors powder used for thermal analysis.

The thermal decomposition and crystallization processes were studied by TG (Netzsch STA 409C) and DSC techniques in an oxygen atmosphere at a heating rate of $10\text{ }^{\circ}\text{C min}^{-1}$. Al_2O_3 was used as reference material during the thermal analysis.

After annealing at $600\text{ }^{\circ}\text{C}$ for 30 min at $10\text{ }^{\circ}\text{C}/\text{min}$ in an electric furnace, the powders were structurally characterized using an automatic X-ray diffractometer (Rigaku, Rotaflex RU200B) with $CuK\alpha$ radiation ($50\text{ kV}, 100\text{ mA}$, $\lambda = 1.5405\text{ \AA}$) and in a θ - 2θ configuration using a graphite monochromator. The scanning range was between 20 and 70 ° (2θ), with a step size of 0.02 ° . Diffuse reflectance and colorimetric coordinates of the pigments were measured in the 400 and 700 nm range, using a spectrophotometer (Minolta, CM2600d) equipped with standard type D65 (day light) light source, following the CIE-L* a^* b^* colorimetric method recommended by the CIE (Commission Internationale de l'Eclairage) [12].

Results and discussion

Figure 1 shows the X-ray diffraction (XRD) patterns of the $Zn_{1-x}M_xO$, with $M = Co, Fe$, and V , samples obtained after heat treatment at $600\text{ }^{\circ}\text{C}$ for 30 min. Comparison of the observed d -values of all the samples with the standard (ICSD file n° 36-1451) clearly revealed the formation of stable monophasic zincite with a hexagonal (wurtzite-type) crystal structure of ZnO .

The cell parameter values for the obtained $Zn_{1-x}M_xO$ powders (Table 1) are comprised between the value $a = b = 3.2498\text{ \AA}$, $c = 5.2066\text{ \AA}$ and $V = 47.62\text{ \AA}^3$ corresponding to wurtzite structure ZnO .

The addition of transition metals induces small changes in the unit cell dimensions. The changes in lattice parameters are in accordance with the metal–oxygen distances due to effective ionic radii of cations [13, 14] (Table 1).

It is well known that metal complexation and polymerization reactions occur during synthesis by the polymeric precursor method [15]. In the material studied here, the complexation of cobalt and zinc with citric acid led to the following reactions:

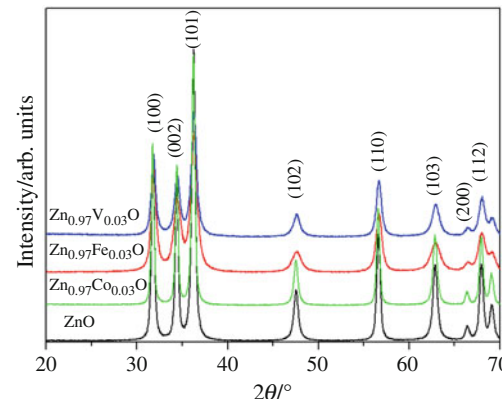
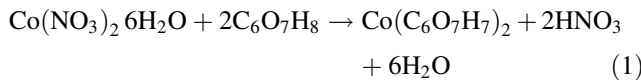


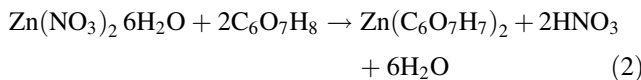
Fig. 1 X-ray diffraction patterns of $Zn_{1-x}M_xO$ ($M = Co, Fe$, and V) samples calcined at $600\text{ }^{\circ}\text{C}/30\text{ min}$

Table 1 Lattice parameter, crystallite size and cell volume of Zn_{1-x}M_xO (M = Co, Fe, and V) samples

Sample	Ionic radii of cations/Å	<i>a</i> = <i>b</i> /Å	<i>c</i> /Å	<i>V</i> /Å ³
ZnO	(Zn ⁺²) 0.74 [6]	3.248	5.205	47.5
Zn _{0.97} Co _{0.03} O	(Co ⁺²) 0.72 [6]	3.247	5.207	47.5
Zn _{0.97} Fe _{0.03} O	(Fe ⁺³) 0.65 [14]	3.249	5.207	47.6
Zn _{0.97} V _{0.03} O	(V ⁺²) 0.79 [20]	3.246	5.208	47.5



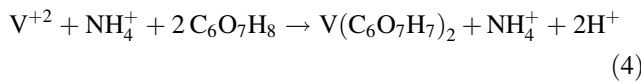
and



forming nitric acid and water. The vanadium complexation reaction occurred in three steps: first the ammonium metavanadate is almost completely dissociated in aqueous solution:

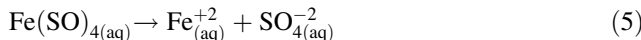


It is well known that in acid medium containing zinc, a fast reduction of vanadium occurs. The solution turn at first blue (VO⁺² ions), then green (V⁺³ ions), and finally violet (V⁺² ions) [16]. In the final step, the vanadium complexation reaction occurred as follows:

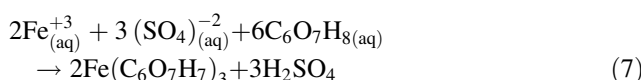


with the formation of ammonium.

The iron complexation reaction must be written in three steps: first, the iron sulfate is almost completely dissociated in aqueous solution, followed by the formation of Fe³⁺ ions since Fe⁺² is readily oxidized in the presence of water and oxygen [17].

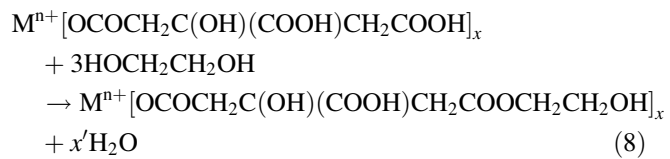


Finally the iron complexation reaction occurred as follows:



with the formation of sulfuric acid.

Mixing these metallic complexes (metallic citrates) above 70 °C triggered the onset of the esterification reaction between metal citrate and ethylene glycol, as follows:



In the compounds studied here, the polyesterification reactions (Eq. 8) occurred continuously until the polymer network was formed. Therefore, the main organic compounds contained in the resin were alcohol, water, ammonium, nitric acid, sulfuric acid, and polyester.

The TG/DSC results presented in Fig. 2 shows the thermal behavior of the Zn_{1-x}M_xO precursor. Organic and other volatile (H₂O, NO_x, CO_x, N_xO_y, etc.) products are lost/removed at temperatures below 440–500 °C. The mass remains constant at higher temperature, indicating oxide formation [18].

The DSC curve shows two exothermic peaks in the 300–500 °C range corresponding to NO_x formation, polymer combustion, and oxidation of other organic residues [18]. These two exothermic peaks are associated with two main events; the lowest temperature is due to pyrolysis of the “puff”, i.e., oxidation of the system, and the highest temperature as a result of the crystallization of the ceramic powder.

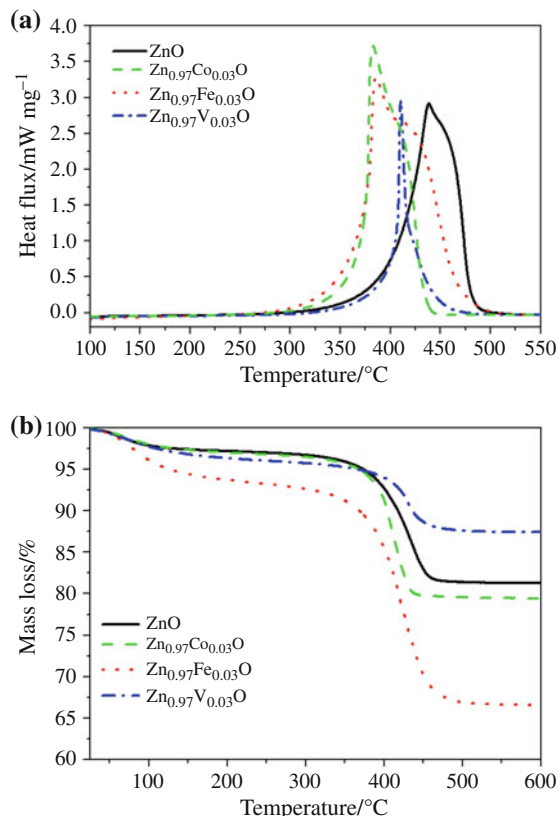


Fig. 2 **a** DSC curves of Zn_{1-x}M_xO (M = Co, Fe, and V) samples and **b** TG curves of Zn_{1-x}M_xO (M = Co, Fe, and V) samples

The peak centered around 400–480 °C refer to pure ZnO samples. In contrast, for samples doped with 3% Co, Fe, and V a shift towards lower temperatures occur. This finding allows us to conclude that the inclusion of transition metals lowers the phase formation temperature to obtain crystalline materials without organic compounds.

ZnO has been worldly used as white inorganic pigment and transition element is known to produce various colors when doped in oxide matrices. This transition element is an efficient coloring agent in glasses and ceramic pigments because of the mobility of its 3d electrons [6].

Qualitative and quantitative information about the color of the samples were obtained using spectral methods. Figure 3 presents the diffuse reflectance spectra for the $Zn_{1-x}M_xO$ samples. Pure ZnO showed an absorption edge around 400 nm. Doped ZnO samples exhibited absorptions in the visible region in addition to the absorption edge due to the bands originating from the crystal-field transitions of transition metals ions replacing Zn in tetrahedral coordination [3].

In the case of Co doped ZnO, three well defined absorption bands at 655, 610, and 568 nm assigned as the Co^{+2} $d-d$ (tetrahedral symmetry) crystal-field transitions $^4A_2(F) \rightarrow ^2A_1(G)$, $^4A_2(F) \rightarrow ^4T_1(P)$ and $^4A_2(F) \rightarrow ^2E_1(G)$, respectively [19]. The absorption around 560 nm for V-doped samples represents typical $d-d$ transition of V^{2+} ions in a tetragonal crystal field [3]. For Fe doped ZnO samples, an absorption band around 480 nm has been attributed to Fe^{3+} in tetrahedral coordination [3]. No significant absorption corresponding to Fe^{2+} ions was observed and so determination of presence of tetrahedral Fe^{2+} by optical spectra was not possible. This result is in agreement with the assumption presented above regarding the oxidation of Fe^{2+} to Fe^{3+} and the reduction of V^{5+} ions to V^{2+} during synthesis.

Table 2 presents the colorimetric coordinates (L^* , a^* , b^*) of $Zn_{1-x}M_xO$ powder systems, using type D65-10°

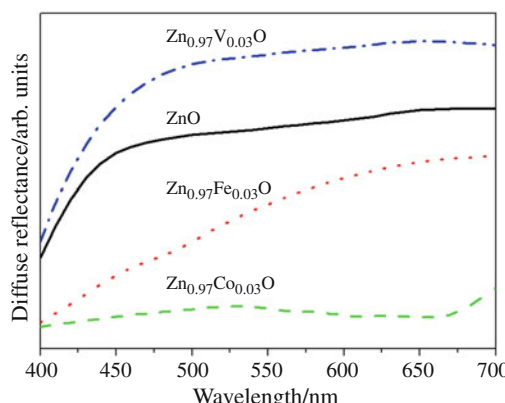


Fig. 3 Diffuse reflectance spectra of $Zn_{1-x}M_xO$ ($M = Co, Fe$, and V) samples calcined at 600 °C/30 min

Table 2 Colorimetric coordinates (L^* , a^* , and b^*) of $Zn_{1-x}M_xO$ ($M = Co, Fe$, and V) powders systems, using light source type D65-10° (day light), following the CIE- $L^*a^*b^*$ standard colorimetric method

Samples	L^*	a^*	b^*
ZnO	81.34	-0.73	8.52
$Zn_{0.97}Co_{0.03}O$	38.22	-12.43	7.22
$Zn_{0.97}Fe_{0.03}O$	78.86	4.39	34.57
$Zn_{0.97}V_{0.03}O$	90.56	-2.95	13.07

(day light) light source, according to the CIE- $L^*a^*b^*$ standard colorimetric method. These colorimetric coordinates must be analyzed simultaneously to determine the final color of pigments, especially the a^* and b^* coordinates. The pure ZnO sample presented a white color. The samples become greenish with cobalt content, yellowish with iron, and a beige color for the ones doped with vanadium was obtained.

Conclusions

The polymeric precursor method proved efficient to synthesize pigments with colors ranging from white (ZnO), green ($Zn_{0.97}Co_{0.03}O$), yellow ($Zn_{0.97}Fe_{0.03}O$), and beige ($Zn_{0.97}V_{0.03}O$). Powders of the system pure ZnO and $Zn_{0.97}M_{0.03}O$ ($M = Co, Fe$, and V) were synthesized as a single phase with wurtzite structure. The DSC and TG techniques allowed to determine the temperature range of processes: degradation of the polymer (pyrolysis of the organic compounds), elimination of nitrates and water, and phase formation. For the powders obtained the inclusion of the different dopants to ZnO lowers the phase formation temperature to obtain crystalline materials without organic compounds. Diffuse reflectance spectra confirmed the assumption regarding the oxidation of Fe^{2+} to Fe^{3+} and the reduction of V^{5+} ions to V^{2+} during synthesis.

Acknowledgements The authors also gratefully acknowledge the financial support of the Brazilian research funding agencies FAPESP, CAPES, and CNPq.

References

- Martos M, Martínez M, Cordoncillo E, Escribano P. Towards more ecological ceramic pigments: study of the influence of glass composition on the colour stability of a pink chromium-doped ceramic pigment. *J Eur Ceram Soc*. 2007. doi:[10.1016/j.jeurceramsoc.2007.03.030](https://doi.org/10.1016/j.jeurceramsoc.2007.03.030).
- Cho S, Jung S-H, Lee K-H. Morphology-controlled growth of ZnO nanostructures using microwave irradiation: from basic to complex structure. *J Phys Chem*. 2008. doi:[10.1021/jp803783s](https://doi.org/10.1021/jp803783s).

3. Singh S, Rama N, Sethupathi K, Rao RMS. Correlation between electrical transport, optical, and magnetic properties of transition metal ion doped Zn. *J Appl Phys.* 2008. doi: [10.1063/1.2834443](https://doi.org/10.1063/1.2834443).
4. Zhang W-H, Zhang W-D, Zhou J-F. Solvent thermal synthesis and gas-sensing properties of Fe-doped ZnO. *J Mater Sci.* 2010. doi: [10.1007/s10853-009-3920-y](https://doi.org/10.1007/s10853-009-3920-y).
5. Ghoshal T, Biswas S, Paul M, De SK. Synthesis of ZnO nanoparticles by solvothermal method and their ammonia sensing propertie. *J Nanosci Nanotechnol.* 2009. doi: [10.1166/jnn.2009.1290](https://doi.org/10.1166/jnn.2009.1290).
6. Lavat AE, Wagner CC, Tasca JE. Interaction of Co-ZnO pigments with ceramic frits: a combined study by XRD, FTIR and UV-visible. *Ceram Inter.* 2008. doi: [10.1016/j.ceramint.2007.09.003](https://doi.org/10.1016/j.ceramint.2007.09.003).
7. Gaudon M, Toulemonde O, Demouragues A. Green coloration of co-doped ZnO explained from structural refinement and bond considerations. *Inorg Chem.* 2007. doi: [10.1021/ic701157j](https://doi.org/10.1021/ic701157j).
8. Lima RC, Macario LR, Espinosa JWM, Longo VM, Erló R, Marana N, Sambrano JR, dos Santos ML, Moura AP, Pizani PS, Andrés J, Longo E, Varela JA. Toward an understanding of intermediate- and short-range defects in ZnO single crystals. A combined experimental and theoretical study. *J Phys Chem.* 2008. doi: [10.1021/jp8022474](https://doi.org/10.1021/jp8022474).
9. Pechini M. Method of preparing lead and alkaline—earth titanates and niobates and coating method using the same to form a capacitor. US Patent 3,330,697. 1967.
10. Kakihana M. Invited review “sol–gel” preparation of high temperature superconducting oxides. *J Sol–Gel Sci Technol.* 1996. doi: [10.1007/BF00402588](https://doi.org/10.1007/BF00402588).
11. Araújo VD, Bernardi MIB. Synthesis and optical and structural characterization of Ce_(1-x)O₂:M_xO (M = Cu, Co) pigments. *J Therm Anal Calorim.* 2010. doi: [10.1007/s10973-010-0892-8](https://doi.org/10.1007/s10973-010-0892-8).
12. CIE. Recommendations of uniform color spaces, color difference equations, phychometrics color terms. Supplement no. 2 of CIE Publ. N°. 15 (E1e1.31) 1971, Bureau Central de la CIE, Paris; 1978.
13. Matteucci F, Cruciani G, Dondi M, Gasparotto G, Tobaldi DM. Crystal structure, optical properties and colouring performance of karrooite MgTi₂O₅ ceramic pigments. *J Solid State Chem.* 2007. doi: [10.1016/j.jssc.2007.08.029](https://doi.org/10.1016/j.jssc.2007.08.029).
14. Dondi M, Matteucci F, Cruciani G, Gasparotto G, Tobaldi DM. Pseudobrookite ceramic pigments: crystal structural, optical and technological properties. *Solid State Sci.* 2007. doi: [10.1016/j.solidstatesciences.2007.03.001](https://doi.org/10.1016/j.solidstatesciences.2007.03.001).
15. Bernardi MIB, Araújo VD, Mesquita A, Frigo GJM, Maia LJQ. Thermal, structural and optical properties of Al₂CoO₄-Crocoite composite nanoparticles used as pigments. *J Therm Anal Calorim.* 2009. doi: [10.1007/s10973-009-0164-7](https://doi.org/10.1007/s10973-009-0164-7).
16. Vogel AI. Textbook of macro and semimacro qualitative inorganic analysis, 5th edn. London: Longman; 1979. p. 527.
17. Roosendaal SJ, Bakker JPR, Vredenberg AM, Habraken FHPM. Passivation of iron in H₂O an O₂/H₂O mixtures. *Surf Sci.* 2001. doi: [10.1016/S0039-6028\(01\)01325-5](https://doi.org/10.1016/S0039-6028(01)01325-5).
18. Fernandes DM, Silva R, Hechenleitner AAW, Radovanovic E, Melo MAC, Pineda EAG. Synthesis and characterization of ZnO, CuO and a mixed Zn and Cu oxide. *Mater Chem Phys.* 2009. doi: [10.1016/j.matchemphys.2008.11.038](https://doi.org/10.1016/j.matchemphys.2008.11.038).
19. Naeem M, Hasanain SK, Mumtaz A. Electrical transport and optical studies of ferromagnetic Cobalt doped ZnO nanoparticles exhibiting a metal-insulator transition. *J Phys Condens Matter.* 2008. doi: [10.1088/0953-8984/20/02/025210](https://doi.org/10.1088/0953-8984/20/02/025210).
20. Shannon RD. Revised effective ionic radii and systematic studies of interatomie distances in halides and chaleogenides. *Acta Cryst.* 1976;A32:751–67.